



Article

# Generation of a Novel Nkx6-1 Venus Fusion Reporter Mouse Line

Ingo Burtscher <sup>1,2,†</sup> , Marta Tarquis-Medina <sup>1,2,3,†</sup>,  
Ciro Salinno <sup>1,2,3</sup>, Silvia Schirge <sup>1,2</sup>, Julia Beckenbauer <sup>1,2</sup>,  
Mostafa Bakhti <sup>1,2</sup> and Heiko Lickert <sup>1,2,3,\*</sup>

- <sup>1</sup> Institute of Diabetes and Regeneration Research, Helmholtz Zentrum München, 85764 Neuherberg, Germany; ingo.burtscher@helmholtz-muenchen.de (I.B.); marta.medina@helmholtz-muenchen.de (M.T.-M.); ciro.salinno@helmholtz-muenchen.de (C.S.); silvia.schirge@helmholtz-muenchen.de (S.S.); julia.beckenbauer@helmholtz-muenchen.de (J.B.); mostafa.bakhti@helmholtz-muenchen.de (M.B.)
- <sup>2</sup> German Center for Diabetes Research (DZD), 85764 Neuherberg, Germany
- <sup>3</sup> School of Medicine, Technische Universität München, 81675 München, Germany
- \* Correspondence: heiko.lickert@helmholtz-muenchen.de
- † These authors equally contributed to this work.

**Abstract:** Nkx6-1 is a member of the Nkx family of homeodomain transcription factors (TFs) that regulates motor neuron development, neuron specification and pancreatic endocrine and  $\beta$ -cell differentiation. To facilitate the isolation and tracking of Nkx6-1-expressing cells, we have generated a novel Nkx6-1 Venus fusion (Nkx6-1-VF) reporter allele. The Nkx6-1-VF knock-in reporter is regulated by endogenous cis-regulatory elements of Nkx6-1 and the fluorescent protein fusion does not interfere with the TF function, as homozygous mice are viable and fertile. The nuclear localization of Nkx6-1-VF protein reflects the endogenous Nkx6-1 protein distribution. During embryonic pancreas development, the reporter protein marks the pancreatic ductal progenitors and the endocrine lineage, but is absent in the exocrine compartment. As expected, the levels of Nkx6-1-VF reporter are upregulated upon  $\beta$ -cell differentiation during the major wave of endocrinogenesis. In the adult islets of Langerhans, the reporter protein is exclusively found in insulin-secreting  $\beta$ -cells. Importantly, the Venus reporter activities allow successful tracking of  $\beta$ -cells in live-cell imaging and their specific isolation by flow sorting. In summary, the generation of the Nkx6-1-VF reporter line reflects the expression pattern and dynamics of the endogenous protein and thus provides a unique tool to study the spatio-temporal expression pattern of this TF during organ development and enables isolation and tracking of Nkx6-1-expressing cells such as pancreatic  $\beta$ -cells, but also neurons and motor neurons in health and disease.

**Keywords:** Nkx6-1; pancreas development; fluorescent reporter; endocrine lineage; secondary transition;  $\beta$ -cells; live imaging



**Citation:** Burtscher, I.; Tarquis-Medina, M.; Salinno, C.; Schirge, S.; Beckenbauer, J.; Bakhti, M.; Lickert, H. Generation of a Novel Nkx6-1 Venus Fusion Reporter Mouse Line. *Int. J. Mol. Sci.* **2021**, *22*, 3434. <https://doi.org/10.3390/ijms22073434>

Academic Editor:  
Michel Aurrand-Lions

Received: 25 February 2021  
Accepted: 22 March 2021  
Published: 26 March 2021

**Publisher's Note:** MDPI stays neutral with regard to jurisdictional claims in published maps and institutional affiliations.



**Copyright:** © 2021 by the authors. Licensee MDPI, Basel, Switzerland. This article is an open access article distributed under the terms and conditions of the Creative Commons Attribution (CC BY) license (<https://creativecommons.org/licenses/by/4.0/>).

## 1. Introduction

The endoderm-derived pancreas comprises exocrine and endocrine compartments that contribute to nutrient digestion and regulate blood glucose homeostasis, respectively. The exocrine pancreas consists of ductal epithelium and acinar cells, whereas the endocrine pancreas is defined by the islets of Langerhans and contains five distinct hormone-producing cell types [1,2]. Among these, insulin-producing  $\beta$ -cells are the most prominent pancreatic endocrine cell type that represents around 80% of the total endocrine population in the mouse adult islets [3,4]. In mice, pancreas organogenesis is initiated by the formation of a dorsal and a ventral pancreatic bud from the foregut endoderm growing into the surrounding mesenchyme at embryonic day 9 (E9.0). The plexus structure of the early buds consists of multipotent progenitor cells (MPCs), which are characterized by the expression of several transcription factors (TFs) including Pdx1, Ptf1 and Nkx6-1. From E9.5 to E12.5, the pancreas undergoes the primary transition, in which progenitor cells

massively proliferate and form a transiently stratified epithelium surrounding microlumen structures. During the secondary transition (E13.5–15.5), the pancreatic epithelium undergoes extensive remodeling to generate a continuous tubular network followed by enormous cell differentiation to produce ductal, acinar and endocrine lineages. At E15.5, the mouse pancreas contains a ramified tubular epithelium, which consists of round tip domains containing acinar progenitors (Ptf1+) and trunk domains (Sox9+). Within the trunk region, bipotent progenitors possess ductal or endocrine fate potential [1,5,6]. Upon differentiation, the endocrine cells leave the ductal epithelium and assemble into clusters to form the islets of Langerhans [7].

The Nkx family of homeodomain factors includes several members, among which Nkx6-1 plays a key role during foregut patterning, pancreas organogenesis and central and peripheral nervous system development. In the ventral neuronal progenitors, Nkx6-1 plays a role in progenitor specification by modulating the neural response to the glycoprotein sonic hedgehog (Shh; [8,9]). In the foregut, Nkx6-1 is expressed in the smooth muscle cells of esophageal and dorsal tracheal mesenchyme and its function is required for promoting smooth muscle development in the esophageal region [10]. During pancreas development, Nkx6-1 plays a key role in pancreatic epithelium patterning. Reciprocal suppression of Nkx6-1 and Ptf1a leads to the formation of the trunk and tip domains, respectively [11,12]. Therefore, upon loss of Nkx6-1, acinar fate is increased [11] at the expense of endocrine cells [13–16]. As the differentiation of bipotent trunk cells towards  $\beta$ -cells proceeds, the levels of Nkx6-1 increase [17]. Together with Pdx1, Nkx6-1 is required for  $\beta$ -cell specification by suppressing the  $\alpha$ -cell program [18,19]. In adult mice, Nkx6-1 is exclusively expressed in  $\beta$ -cells [20] to maintain their identity and proper insulin secretion [19,21]. Lack of Nkx6-1 in mature  $\beta$ -cells leads to rapid onset of diabetes caused by defects in insulin biosynthesis and secretion without affecting cell survival [21]. Furthermore, diminished expression of NKX6-1 is associated with the development of Type 2 Diabetes (T2D) in humans and rodents [22,23]. In addition, three genome-wide association studies (GWASs) have identified NKX6-1 variants associated with T2D [24–26], further suggesting the importance of this TF for human  $\beta$ -cell formation and function.

Here, we report the generation of a novel reporter mouse line, in which the bright fluorescent protein Venus is fused to the C-terminus of the endogenous Nkx6-1. The homozygous reporter mice are viable and fertile. The Nkx6-1-Venus fusion (Nkx6-1-VF) protein follows the spatio-temporal expression pattern of endogenous Nkx6-1 during pancreas development and in adult islets. Moreover, the expression of Venus enables one to track  $\beta$ -cells in live imaging and isolate them specifically by flow cytometry. Thus, the Nkx6-1-VF mouse line provides a unique tool to study Nkx6-1 expression and function during organ development as well as  $\beta$ -cell function in health and disease.

## 2. Results and Discussion

### 2.1. Generation of the Nkx6-1-VF Mouse Line

The Nkx6-1-VF mouse line was generated by CRISPR/Cas9-mediated double strand breaks followed by homologous recombination. Using a targeting vector as template DNA for directed repair resulted in the generation of an Nkx6-1-VF reporter gene under control of the endogenous Nkx6-1 cis-regulatory elements (Figure 1a). To do so, we designed a targeting vector by standard cloning techniques by removing the translational stop codon of the Nkx6-1 gene in exon 3 and generating an in-frame fusion transcript with the Venus open reading frame and a Flag tag. For selection purposes, a loxP-flanked phosphoglycerate kinase (PGK) promoter-driven neomycin (Neo) resistance gene in the opposite orientation was inserted after the reporter gene. After removal of the Neo selection marker, the Nkx6-1-VF mRNA transcript utilizes the endogenous untranslated region (UTR). The targeting vector, Cas9D10A expression vector and two guide RNA vectors expressing guide RNAs that bind shortly before and after the Nkx6-1 stop codon were electroporated into F1 hybrid (129Sv/Bl6) IDG3.2 embryonic stem (ES) cells. Neomycin-resistant clones were screened with 5' and 3' homology arm spanning PCRs (Figure 1b,c). Germline

chimeras of the Nkx6-1-VFNeo mouse line were generated from two independent ES cell clones by ES cell aggregation with CD1 morulae. The loxP-flanked Neo selection cassette was deleted in the germline by Cre recombination-mediated excision (Figure 1d; [27]) resulting in the Nkx6-1-VF mouse line. Heterozygous animals were intercrossed and genotyped for all possible alleles (Figure 1e). From 9 litters with a total of 59 animals, 40% were heterozygous, 27% homozygous and 32% wild type, following the expected Mendelian ratio. No embryonic phenotype was observed and offspring homozygous for the Nkx6-1-VF allele were viable and appeared indistinguishable from their wild-type littermates. To confirm if the Nkx6-1-VF reporter was properly synthesized and reflected endogenous Nkx6-1 protein, we performed Western blot analysis using lysates from islets of Langerhans from WT, heterozygous and homozygous reporter mice. The Nkx6-1 WT protein was detected as a double band at 50 and 53 kDa with the anti-Nkx6-1 antibody (Figure 1f). This double band was also observed with the Nkx6-1-VF protein, appearing as a double band at approximately 77 and 80 kDa using anti-Nkx6-1, anti-GFP and anti-Flag antibodies (Figure 1f–h) but we also detected degradation products at 40 and 55 kDa. Both the Nkx6-1 and Nkx6-1-VF protein were synthesized in comparable ratios, as revealed by anti-Nkx6-1 antibody in lysates from heterozygous animals (Figure 1f). In summary, we have shown that the Nkx6-1-VF reporter is correctly integrated in the genome and the transcription factor is functional, as homozygous offspring are viable. Furthermore, we showed that the reporter is translated as a fusion protein and can be detected with Flag and Venus antibodies.

## *2.2. Spatio-Temporal Expression Pattern of Nkx6-1-VF Protein during Embryonic Pancreas Development*

To assess whether the Nkx6-1-VF protein reflects the expression pattern of the endogenous Nkx6-1 protein, we stained embryos and embryonic pancreatic sections from the reporter mice. At E9.5, Venus expression was detected in pancreatic buds marked by high expression of Pdx1 and Foxa2 (Figure 2a; yellow arrows) as well as in the neural tube (Figure 2a; white arrows) as previously reported [8]. At 11.5, Nkx6-1-VF is co-expressed with the TF Pdx1 in the pancreatic epithelium. Interestingly Nkx6-1-VF was found in both pancreatic buds (Figure 2c), whereas it was absent in the first appearing glucagon-secreting endocrine cells during the primary transition (Figure 2b). In pancreatic sections of E12.5 embryos, the Venus fusion protein localized in the cell nucleus and was restricted to the trunk domain of epithelium (Figure 2d; yellow arrow). In pancreatic sections of E12.5 embryos, Venus showed nuclear expression and was highly expressed in the Pdx1-positive trunk of the epithelium, whereas expression was low or absent in the tip domain. Correctly patterned tip and trunk domains indicate that the Nkx6-1-VF does not impair transcription factor function and allows correct patterning of the pancreatic epithelium (Figure 2d; white arrows). The co-expression of Nkx6-1-VF and Pdx1 was also observed at E16.5 and E18.5. At stage E16.5, we found low expression of the fusion protein in epithelial cells defined by the expression of E-cadherin (Figure 2e; purple arrows). Additionally, Nkx6-1-VF was expressed at higher levels in certain cell populations in close proximity to the ductal epithelium that resembled proto-islets (Figure 2e; white arrows). Finally, we confirmed the colocalization within the nuclei of Nkx6-1 and Venus markers at E18.5 (Figure S1). Overall, these results demonstrate that the Nkx6-1-VF protein mirrors the endogenous Nkx6-1 spatio-temporal expression pattern during pancreas development.

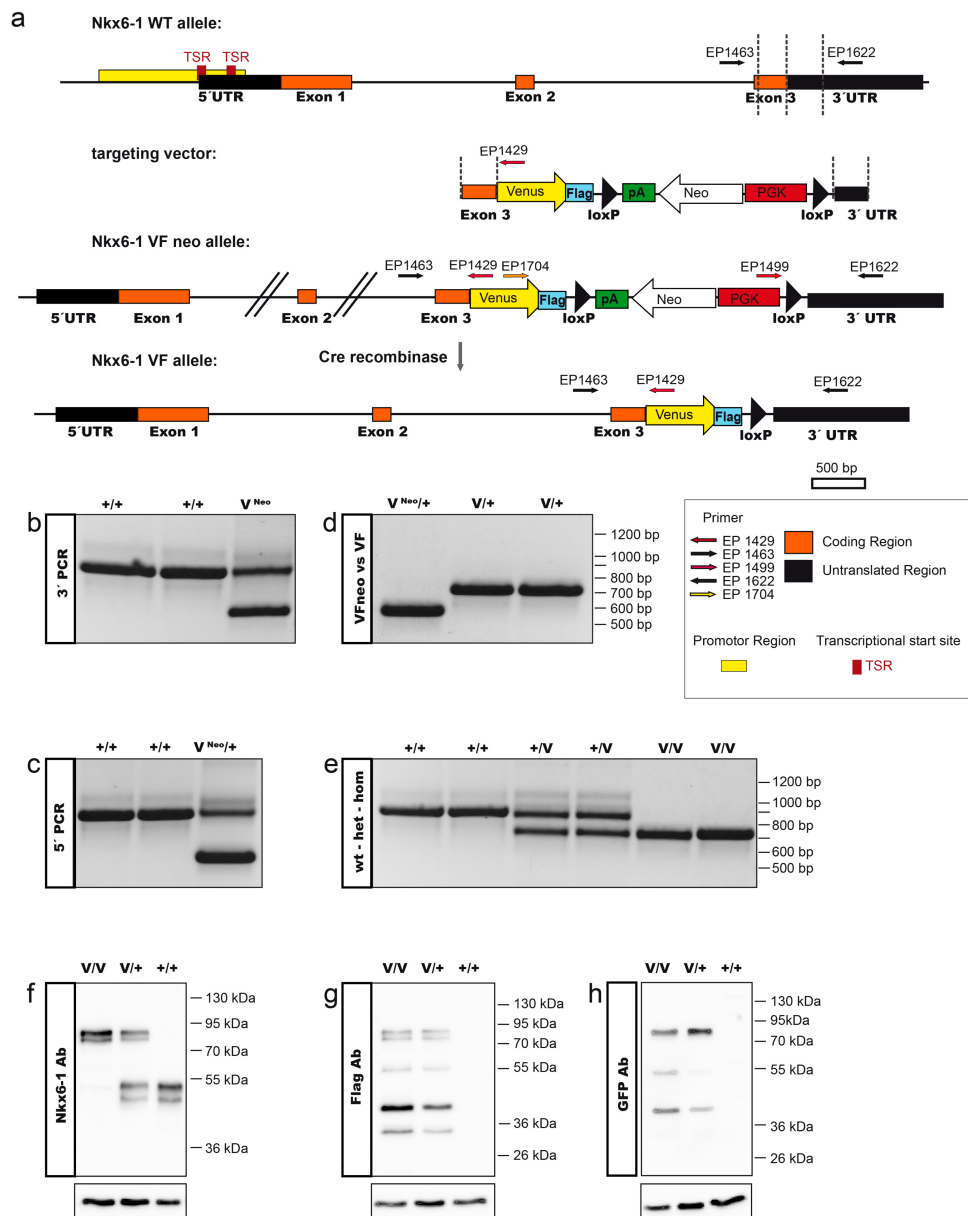


**Figure 1.** Generation of the Nkx6-1 Venus fusion (Nkx6-1-VF) allele. **(a)** Targeting strategy for the Nkx6-1-VF allele. A double strand break was introduced by two nicks of the D19A mutant Cas9 using two gRNAs (green arrows) binding before and after the stop codon of Nkx6-1. A targeting vector was used to repair the gap and fuse the coding region of the fluorescent report gene Venus to the open reading frame (orange boxes) of the Nkx6-1 gene. The loxP-flanked PGK-driven neomycin (Neo) selection cassette was removed by Cre recombinase-mediated excision. Nkx6-1 5' and 3' untranslated regions (UTRs) are indicated by black boxes, the predicted promoter region (yellow box) and transcriptional start sites (TSR, red boxes) are indicated. Primers used for PCR genotyping are designated EP1429, EP1463, EP1499, EP1622 and EP1704. The positions of the homology regions to generate the targeting construct are indicated by dashed lines. **(b,c)** PCR genotyping of Nkx6-1-VFNeO/+ mice using primers 1429, EP1463, EP1622 for the 5' PCR confirmation of the targeted allele Nkx6-1-VFNeO (545 bp) versus the WT allele (877bp) and the primers EP1463, EP1499 and EP1622 for the 3' PCR confirmation of the targeted allele Nkx6-1-VFNeO (591 bp) versus the WT allele (877bp). **(d)** PCR primers EP1499, 1622 and 1704 were used to distinguish the allele before (Nkx6-1-VFNeO; 591 bp) and after removal of the Neo selection cassette (Nkx6-1-VF; 741 bp). **(e)** Primers EP1463, EP1622 and EP1704 were used to distinguish WT from heterozygous or homozygous mice of Nkx6-1-VF resulting in 877bp for the WT allele and 741 bp for the targeted allele. **(f)** Western blot analysis on lysates from islets of Langerhans using Nkx6-1 antibody to detect the WT protein as double band at approximately 50 and 53 kDa and Nkx6-1-VF protein at 77 and 80 kDa. **(g,h)** Both Flag and GFP antibodies detected the Nkx6-1-Venus fusion protein at 77 and 80 kDa as well as several degradation products.  $\beta$ -tubulin was used for loading control.



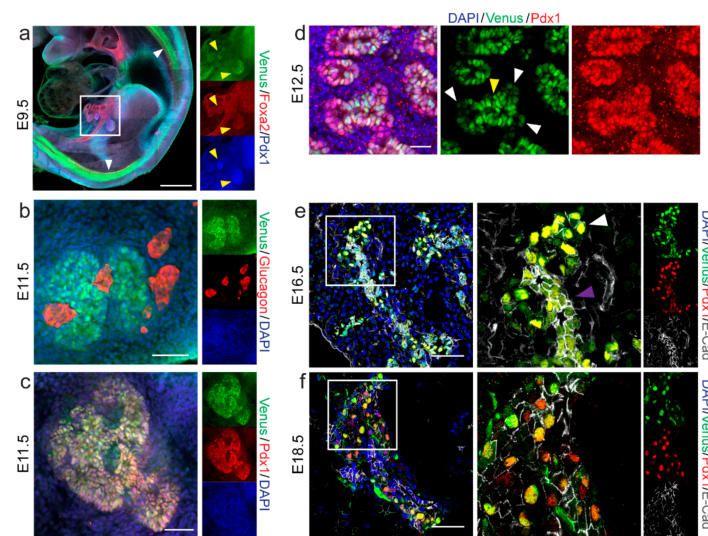


**Figure 2.** Nkx6-1-VF expression during embryonic pancreas development. (a) Whole embryo immunostaining using iDISCO protocol of E9.5 presenting Nkx6-1-VF expression in notochord (white arrows) and pancreatic buds marked by high expression of Pdx1 and Foxa2 (yellow arrows). Tile scan; size bar 500  $\mu\text{m}$ . (b,c) Whole pancreas immunostaining at stage E11.5 shows (c) colocalization of Nkx6-1-VF and Pdx1 in the pancreatic epithelial but (b) is absent in the glucagon-secreting cells. Scale bar 50  $\mu\text{m}$ . (d–f) Pancreas section immunostaining of E12.5, E16.5 and E18.5 analyzing the expression of Nkx6-1-VF during embryonic pancreas development. The expression of the fusion protein through primary and secondary transition follows a similar pattern to Pdx1. (d) At E12.5, the expression of Nkx6-1-VF is observed in the duct domain (yellow arrow) but not in the tip domain (white arrow). Scale bar 20  $\mu\text{m}$ . (e,f) During endocrine lineage specification, higher expression levels outside the duct marked with high expression of membrane marker E-cadherin is observed. Scale bar 50  $\mu\text{m}$ .

### 2.3. Nkx6-1-VF Marks the Endocrine Lineage during Secondary Transition

During the secondary transition of pancreas development, the expression of Nkx6-1 is found in the ductal epithelium and endocrine progenitor cells. As endocrine cells differentiate, the levels of Nkx6-1 increase and its expression becomes restricted to  $\beta$ -cells [17]. Therefore, we evaluated the expression pattern of Nkx6-1-VF in pancreatic sections at E16.5 and E18.5, when endocrinogenesis occurs. Using immunohistochemical analysis, we found low expression levels of Nkx6-1-VF in Sox9<sup>+</sup> ductal cells and high expression of the fusion protein in a Sox9<sup>+</sup> cell clusters close to the trunk epithelium (Figure 3a–c). To define the identity of the latter population, we performed co-staining of Nkx6-1-VF with glucagon and insulin to identify  $\alpha$ - and  $\beta$ -cells, respectively, in E18.5 pancreatic sections. The results indicate that at E18.5, Nkx6-1-VF was expressed at high levels in  $\beta$ -cells, whereas in  $\alpha$ -cells reporter expression was strongly downregulated (Figure 3d,e). Furthermore, co-staining of the fusion protein with the exocrine marker  $\alpha$ -amylase revealed no expression of the Nkx6-1-VF protein in the exocrine compartment (Figure 3f). Collectively, these data confirm that the expression of Nkx6-1-VF protein becomes restricted from ductal bipotent progenitors to  $\beta$ -cells during secondary transition of pancreas development.

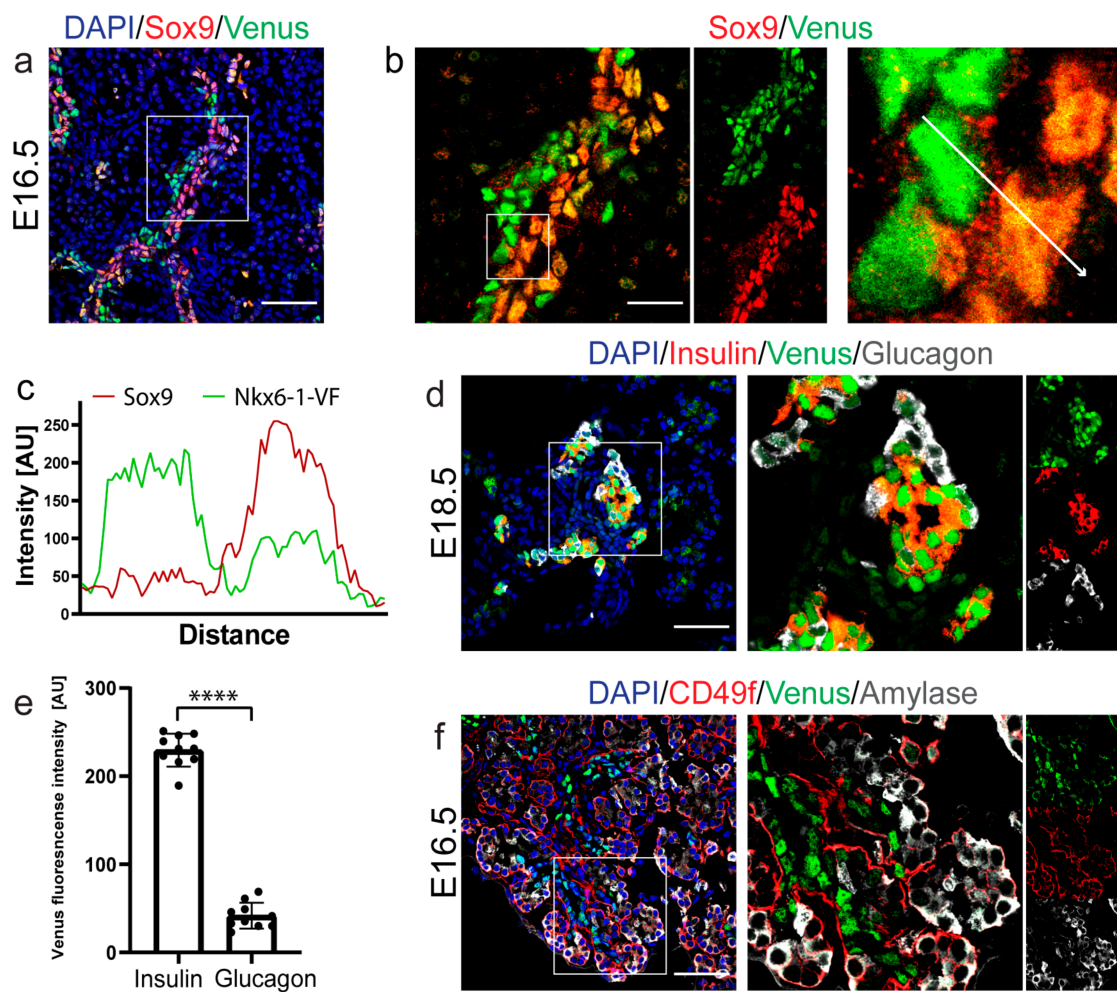


**Figure 3.** Nkx6-1-VF marks the endocrine lineage during secondary transition. (a,b,f) Immunostaining of E16.5 and (d) E18.5 pancreas section exhibiting Nkx6-1-VF expression during endocrine cell formation and  $\beta$ -cell lineage specification. Scale bar 50  $\mu$ m. (b) Immunostaining analysis of E16.5 pancreas (scale bar 20 $\mu$ m) shows that Nkx6-1-VF expression is expressed (c) at low levels in the duct (Sox9+/Nkx6-1-VF low) and high levels near the duct (Sox9-/Nkx6-1-VF high), (f) but not in the exocrine cells marked by amylase. (d,e) At E18.5, the Nkx6-1-VF high expression levels correlate with endocrine lineage formation and mark insulin-secreting cells. Scale bar 50  $\mu$ m. \*\*\*  $p < 0.0001$ ;  $t$ -test.

#### 2.4. Nkx6-1-VF Expression Pattern in the Adult Pancreas

In adult islets, Nkx6-1 is exclusively expressed in  $\beta$ -cells and not in any other endocrine cell types [20]. To investigate whether the Nkx6-1-VF reporter also remains restricted to  $\beta$ -cells in postnatal and adult stages in islet of Langerhans, we performed immunostaining of sections derived from adult pancreas or isolated islets. We co-stained the sections with antibodies against Venus, insulin and Nkx6-1. Venus expression was highly co-localizing with Nkx6-1 in the nucleus (Figure 4a,f), but low Venus levels were also found within the cytoplasm of  $\beta$ -cells (Figure 4a). Weak cytoplasmatic localization of Nkx6-1 reporter in  $\beta$ -cells was not detected by Nkx6-1 antibody (Figure 4a) and was likely caused by protein degradation and immunoreactive Venus fragments [28] which we also observed in the Western blot results (Figure 1h). The specific expression of Nkx6-1-VF protein in  $\beta$ -cells was further confirmed by co-staining of Venus with glucagon, indicating the absence of Venus nuclear signal in  $\alpha$ -cells (Figure 4b). In addition, we analyzed the expression of the  $\beta$ -cell maturation marker, Urocortin 3 (Ucn3) in the Nkx6-1-VF-expressing cells. At postnatal day 3 (P3), when the majority of  $\beta$ -cells were still immature, we found the expression of Ucn3 only in a fraction of Nkx6-1-VF-expressing cells (Figure 4c). On the

contrary, at P45, all the Nkx6-1-VF+ cells expressed Ucn3 (Figure 4d), indicating that the fusion reporter protein does not hamper  $\beta$ -cell maturation. Next, we performed time-lapse imaging of isolated islets derived from Nkx6-1-VF mice. Fluorescent intensity of the Nkx6-1-VF reporter was sufficient to track single  $\beta$ -cells during time-lapse imaging and to follow  $\beta$ -cell movement (Figure 4e; Supplementary movie). Additionally, as the Nkx6-1-VF mRNA uses the endogenous Nkx6-1 UTR, it may be used as a sensor to study miRNA function. Finally, we successfully sorted Nkx6-1-VF+ cells from the isolated adult islets using Fluorescence-activated Cell Sorting (FACS; Figure 4g), indicating the capability of the fusion reporter protein for specific isolation of  $\beta$ -cells.

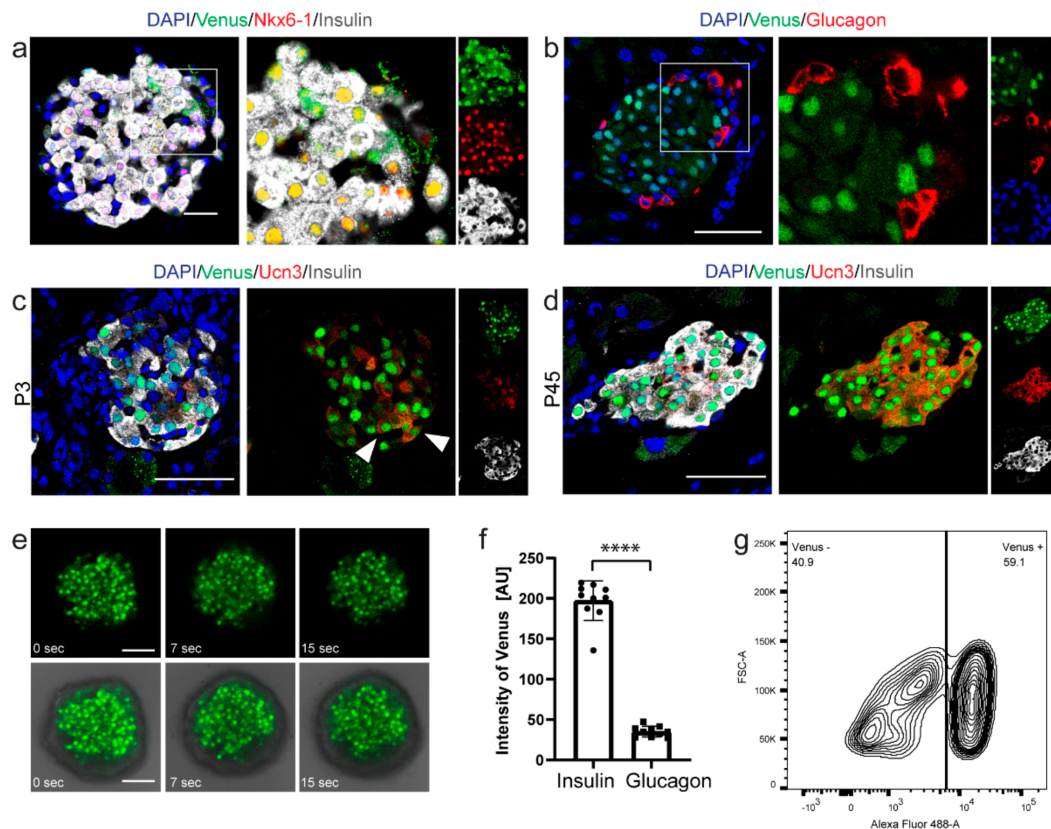


**Figure 4.** Nkx6-1-VF adult mice express Venus in the mature islets and can be used to sort  $\beta$ -cells in vivo. (a) Co-staining of GFP and Nkx6-1 on heterozygous adult pancreatic islets shows co-localization of both markers in insulin-producing cells (b,f) but no expression in glucagon-secreting cells. (c,d) Immunostaining of P3 and P45 pancreatic sections showing the maturation of Nkx6-1-VF  $\beta$ -cells. (c) At P3, only a fraction (white arrowheads) of the reporter cells express Ucn3, (d) while all the reporter cells express this maturation marker at P45. Scale bar 50  $\mu$ m. (e) Time-lapse imaging of isolated islets from adult Nkx6-1-VF mice. Scale bar 50  $\mu$ m. (g) Representative FACS-plot indicating the successful separation of endocrine cells from the isolated adult islets based on the Venus fluorescent signal. \*\*\*  $p < 0.0001$ ;  $t$ -test.

In summary, we have generated the first Nkx6-1-Venus fusion reporter mouse model that resembles the expression of endogenous Nkx6-1 and provides a unique tool for isolation of Nkx6-1-expressing pancreatic cells at different stages. As such, the Nkx6-1-VF reporter protein can be used to quantify the Nkx6-1 protein levels, to analyze cell-fate decisions in time-lapse studies and purify cell populations by FACS, but also to analyze microRNA effects on the UTR using the Venus reporter as a live sensor for protein translation. Therefore, this mouse line offers a valuable technical support to study pancreas development and  $\beta$ -cell function in health and disease.



### 3. Materials and Methods

#### 3.1. Generation of the Targeting Construct

For the targeting vector, the 5' homology region (HR) and 3' HR were PCR amplified using C57B16 BAC (RPCIB-731L18311Q) as a template and using the following primers: EP\_1197 and EP\_1198 primers (see Table S1) for 5' HR and EP\_1199 and EP\_1200 primers for 3' HR. 5' HR was subcloned via NotI and XbaI and 3' HR was subcloned via HindIII and XhoI, into the pBluescript KS (pBKS), generating the pBKS-Nkx6-1 Ex3-HR. Using primers EP\_1126 and EP\_1201 on a Venus-containing DNA template, a Venus-3xFlag tag fragment (819 bp) was amplified and gel purified after XbaI and SpeI digestion and subcloned between 5' and 3' HRs, resulting in pBKS-Nkx6-1 Ex3-HR-Venus-3xFlag. The PGK promoter-driven neomycin resistance gene flanked by loxP sites (loxP-Neo-loxP) was released by BamHI and EcoRI digestion from the PL452-loxP [29] and cloned into these sites downstream of the Venus gene, resulting in the targeting vector pBKS-Nkx6-1 Ex3-HR-Venus3xFlag-Neo. Two gRNA sequences targeting up- and downstream near the stop codon of Nkx6-1 (Figure 1a) were selected using online CRISPR resources [30]. To generate CRISPR expression vectors, self-annealed oligos (Nkx6-1 Crispr #11 and #16 fwd and rev; Table S1) duplexes with BbsI overhangs were cloned into BbsI-digested pBS-U6-chimericRNA (a generous gift from O. Ortiz, Institute of Developmental Genetics, Helmholtz Zentrum München), resulting in pBS-U6-chimericRNA Nkx6-1 #11 and #16. Successful integration of CRISPRs into pbs-U6-chimericRNA vectors was confirmed by sequencing.

#### 3.2. Cell Culture and Homologous Recombination in ES Cells and Mouse Generation

Mouse ES cells were cultured on a murine embryonic feeder (MEF) layer in Dulbecco's modified Eagle's medium (DMEM, Invitrogen, Carlsbad, CA) containing 15% fetal calf serum (FCS, PAN, Aidenbach, Germany), 2 mM L-glutamine (Life Technologies, Darmstadt, Germany, 200 mM), non-essential amino acids (Invitrogen, Carlsbad, CA, 1003), 100 µM β-mercaptoethanol (Life Technologies, Darmstadt, Germany, 50 mM) and 1500 U/mL leukemia inhibitory factor (LIF, Millipore, Darmstadt, Germany, 107 U/mL). Cells were split every two days using trypsin (0.05% trypsin, 0.53 mM EDTA; Life Technologies, Darmstadt, Germany). IDG 3.2 ES cells [31] were electroporated with a mixture of pBKS-Nkx6-1 Ex3-HR-Venus3xFlag-Neo targeting vector and both pBS-U6-chimericRNA Nkx6-1#11 and #16 as well as Cas9 nickase overexpression vector (pCAG Cas9v2D10A-bpA; a generous gift from O. Ortiz, Institute of Developmental Genetics, Helmholtz Zentrum München). Neo-resistant clones were selected using 300 µg/mL G418 (Life Technologies, Darmstadt, Germany, 50 mg/mL). Homologous recombination at the Nkx6-1 locus was confirmed by homology arm spanning PCRs. Homologous recombined ES cell clones were aggregated with CD1 morulae and the resulting chimeras gave germline transmission of the Nkx6-1-VFNeo allele. The floxed Neo selection marker cassette was deleted in the germ line by intercrossing with the ROSA-Cre mouse line. The Nkx6-1-VF mouse colony was backcrossed to C57BL/6J for a minimum of 8 generations. The average litter size of heterozygous intercrosses was 6.5 animals per litter (N = 9) and homozygous intercrosses gave on average 6.1 pups per litter (N = 11). The mice were kept at the central facilities at Helmholtz Center Munich (HMGU) under Specific-pathogen-free (SPF) conditions. Animal rooms had a light cycle of 12/12 h, temperature of 20–24 °C and humidity of 45–65%. Mice received sterile filtered water and standard diet for rodents ad libitum. The mouse line will be available to the research community upon direct request to H.L.

#### 3.3. Genotyping

Mice genotyping was assessed by PCR analysis of ear clip-derived DNA as a template. The excision of the Neo cassette was confirmed through the genotyping of PCR using the primers EP 1499, 1622 and 1704, generating a 591 bp product for the Nkx6-1Venus Neo allele and a 741 bp product for the Venus delta Neo allele (Figure 1b). To genotype the homozygous and heterozygous Nkx6-1-VF mice, PCR analysis was performed at a 60 °C

annealing temperature using the primers EP 1463, 1622 and 1704. The WT mice (+/+) generated an 877 bp PCR product, distinguished from the 741 bp band of the homozygous mice (*v/v*). Two products of 877 and 741 bp were identified for the heterozygous mice (*v/+*) (Figure 1b).

### 3.4. Western Blot Analysis

Western blot analysis was performed according to the standard protocols. Briefly, lysates from pancreatic islets of Langerhans were subjected to the SDS-PAGE electrophoresis and transferred to the nitrocellulose membranes. After blocking, the membranes were incubated with anti-GFP (rabbit 1:2000; Thermo Scientific, Darmstadt, Germany, A11122), anti-Nkx6-1 (goat 1:300; R&D Systems, Minneapolis, MN, U.S.A., AF5857), anti-Flag (mouse HRP 1:10,000; Sigma, Munich, Germany, A8592) and anti-GAPDH (mouse 1 µg/mL; Merck/Millipore, Darmstadt, Germany). HRP-conjugated secondary antibodies were used as follows: anti-mouse HRP (1:10,000; Millipore, Darmstadt, Germany, 12-349), anti-rabbit HRP (1:10,000; Dianova, Hamburg, Germany, 111-035-046) and anti-goat HRP (1:10,000; Dianova, Hamburg, Germany, 305-035-045). The signals were detected by enhanced chemiluminescence (Thermo Scientific, Darmstadt, Germany).

### 3.5. Pancreas Dissection

Embryonic or adult pancreata were dissected and fixed in 4% Paraformaldehyde (PFA) in Phosphate-buffered saline (PBS) for 2 h at RT. The tissues were then cryoprotected in 10% and 30% sucrose solutions for 2 h at RT and finally incubated in 30% sucrose and tissue-embedding medium (Leica, Munich, Germany) (1:1) at 4 °C overnight. Afterwards, they were embedded in a tissue-freezing medium (Leica, Munich, Germany) and stored at −80 °C. Sections of 20 µm thickness were cut from each sample, mounted on a glass slide (Thermo Fisher Scientific, Darmstadt, Germany) and dried for 10 min at room temperature before use or storage at −20 °C. All animals used were homozygous unless stated otherwise.

### 3.6. Immunostaining of Sections

Cryosections were rehydrated with 1x PBS and permeabilized with 0.2% Triton X-100 in 0.1 M glycine solution for 30 min. Samples were then incubated in a blocking solution (10% FCS, 3% donkey serum, 0.1% bovine serum albumin (BSA) and 0.1% Tween-20 in PBS) for 1 h at RT. Afterwards, primary antibodies diluted in blocking solution were added to the samples overnight at 4 °C. The following primary antibodies were used for staining: anti-Ucn3 (rabbit 1:300; Phoenix Pharmaceuticals, Karlsruhe, Germany, H-019-29), anti-glucagon (guinea pig 1:2500; TAKARA, Saint-Germain-en-Laye, France M182), anti-GFP (chicken 1:1000; Aves Lab, Tigard, OR, U.S.A.; GFP-1020), anti-insulin (rabbit 1:300, Cell signaling, Frankfurt, Germany, 3014), goat anti-Pdx1 (goat 1:300; Abcam, Berlin, Germany, AB47383), anti-E-cadherin (rat 1:300; Santa Cruz, Dallas, TX, U.S.A., SC-59778), anti-Cd49f (rat 1:300; BD 555734), anti-Sox9 (rabbit 1:300; Abcam, Berlin, Germany, AB5535), anti-amylase (rabbit 1:300; Abcam, Berlin, Germany, AB21156), anti-Nkx6-1 (goat 1:200; R&D Systems, Minneapolis, MN, U.S.A., AF5857). Primary antibodies were washed with 1x PBS and secondary antibodies diluted in blocking solution were added for 4 h at RT: anti-rabbit 555 (1:800; Scientific, Darmstadt, Germany A31572), anti-chicken Cy2 (1:800; Dianova, Hamburg, Germany, 703-225-155), anti-guinea pig 649 (1:800; Dianova, Hamburg, Germany; 706-495-148), anti-rat DyLight 549 (1:800; Dianova, Hamburg, Germany, 712-505-153) and anti-goat 555 (1:800; Thermo Scientific, Darmstadt, Germany, A21432). Images were obtained with a Leica microscope of the type DMI 6000 using the LAS AF software. Images were analyzed using LAS AF and ImageJ (v.1.51 23) software programs.

### 3.7. Islet Isolation

Islet isolation was performed by digestion of adult pancreas, as described previously [32]. Collagenase P (Sigma-Aldrich, Munich, Germany) dissolved in Hanks' bal-



anced salt solution (HBSS) with  $\text{Ca}^{2+}/\text{Mg}^{2+}$  was injected into the bile duct to perfuse the pancreas. After a gradient preparation (5 mL 10% RPM + 3 mL 40% Optiprep/per sample), islets were handpicked and incubated at 37 °C 5%  $\text{CO}_2$  in culture with 11 mM glucose in RPMI medium 1640 supplemented with 10% (*v/v*) heat inactivated FBS, 1% (*v/v*) penicillin and streptomycin.

### 3.8. FACS Analysis

Islets from adult Nkx6-1-VF homozygous mice were disaggregated into single cells with TriPLE for 10 min at 37 °C and resuspended in FACS buffer (PBS with FCS 10%) and filtered through a 35 mm cell strainer. Cells were analyzed and isolated using an Aria III (BD Biosciences, Heidelberg, Germany).

### 3.9. Time-Lapse Live Imaging

Time-lapse imaging was carried out as described by Burtscher and Lickert (2009) [33]. Islets were incubated in RPMI medium 1640 supplemented with 10% (*v/v*) heat inactivated FBS, 1% (*v/v*) penicillin and streptomycin cultured on glass-bottom dishes in a 37 °C incubator with 5%  $\text{CO}_2$ . To avoid evaporation, the medium was covered with mineral oil. Image acquisition was performed on a Leica DMI 6000 confocal microscope equipped with an incubation system and image analysis was carried out using Leica LAS AF software.

### 3.10. iDisco for Clearing of Mouse Embryos

E9.5 mouse embryos were processed according to the published iDisco protocol [34]. Primary antibodies were incubated for 5 days, secondary antibodies for 4 days at 37 °C. The following primary antibodies were used for staining: anti-GFP (goat 1:500, Biotrend, Köln, Germany; 600-101-215), anti-Foxa2 (mouse 1:500; Millipore, Darmstadt, Germany, 17-10258), anti-Pdx1 (rabbit 1:500; Cell Signaling, Danvers, MS, U.S.A.; D59H3), and secondary antibodies: anti-goat 488 (1:800; Thermo Scientific, Darmstadt, Germany, A11055), anti-mouse CY5 (1:800; Dianova, Hamburg, Germany; 715-175-151) and anti-rabbit 555 (1:800; Thermo Scientific, Darmstadt, Germany, A31572). Images were taken using tile scan mode on a Zeiss LSM 880 using ZenBlack software 2.0.

**Supplementary Materials:** The following are available online at <https://www.mdpi.com/article/10.3390/ijms22073434/s1>, Figure S1: Venus expression marks Nkx6-1-VF expressing cells at embryonic stage; Table S1: Primer sequences; Video S1: Nkx6-1-VF movie GFP; Video S2: Nkx6-1-VF movie BF + GFP.

**Author Contributions:** Conceptualization, I.B., M.T.-M. and H.L.; Funding acquisition, H.L.; Methodology, I.B., M.T.-M., C.S., S.S., J.B. and M.B.; Supervision, H.L.; Writing—original draft, I.B., M.T.-M. and M.B.; Writing—review and editing, C.S., S.S. and H.L. All authors have read and agreed to the published version of the manuscript.

**Funding:** This work was supported by the Helmholtz-Gemeinschaft (Helmholtz Portfolio Theme Metabolic Dysfunction and Common Disease) and Deutsches Zentrum für Diabetesforschung (DZD).

**Institutional Review Board Statement:** The study was conducted in agreement with the German animal welfare legislation with the approved guidelines of the Society of Laboratory Animals (GV-SOLAS) and the Federation of Laboratory Animals Science Associations (FELASA).

**Informed Consent Statement:** Not applicable.

**Data Availability Statement:** Not applicable.

**Acknowledgments:** We thank Jessica Jaki, Aimée Bastidas-Ponce and Lisa Appel for their technical support.

**Conflicts of Interest:** The authors declare no conflict of interest.

## References

1. Pan, F.C.; Wright, C. Pancreas organogenesis: From bud to plexus to gland. *Dev. Dyn.* **2011**, *240*, 530–565. [[CrossRef](#)] [[PubMed](#)]
2. Shih, H.P.; Wang, A.; Sander, M. Pancreas organogenesis: From lineage determination to morphogenesis. *Annu. Rev. Cell Dev. Biol.* **2013**, *29*, 81–105. [[CrossRef](#)] [[PubMed](#)]
3. Brissova, M.; Fowler, M.J.; Nicholson, W.E.; Chu, A.; Hirshberg, B.; Harlan, D.M.; Powers, A.C. Assessment of human pancreatic islet architecture and composition by laser scanning confocal microscopy. *J. Histochem. Cytochem.* **2005**, *53*, 1087–1097. [[CrossRef](#)] [[PubMed](#)]
4. Roscioni, S.S.; Migliorini, A.; Gegg, M.; Lickert, H. Impact of islet architecture on  $\beta$ -cell heterogeneity, plasticity and function. *Nat. Rev. Endocrinol.* **2016**, *12*, 695–709. [[CrossRef](#)]
5. Bastidas-Ponce, A.; Scheibner, K.; Lickert, H.; Bakhti, M. Cellular and molecular mechanisms coordinating pancreas development. *Development* **2017**, *144*, 2873–2888. [[CrossRef](#)]
6. Villasenor, A.; Chong, D.C.; Henkemeyer, M.; Cleaver, O. Epithelial dynamics of pancreatic branching morphogenesis. *Development* **2010**, *137*, 4295–4305. [[CrossRef](#)]
7. Kesavan, G.; Lieven, O.; Mamidi, A.; Öhlin, Z.L.; Johansson, J.K.; Li, W.-C.; Lommel, S.; Greiner, T.U.; Semb, H. Cdc42/N-WASP signaling links actin dynamics to pancreatic cell delamination and differentiation. *Development* **2014**, *141*, 685–696. [[CrossRef](#)]
8. Li, Y.; Tzatzalos, E.; Kwan, K.Y.; Grumet, M.; Cai, L. Transcriptional regulation of notch1 expression by Nkx6.1 in neural stem/progenitor cells during ventral spinal cord development. *Sci. Rep.* **2016**, *6*, 38665. [[CrossRef](#)]
9. Prakash, N.; Puelles, E.; Freude, K.; Trümbach, D.; Omodei, D.; Di Salvio, M.; Sussel, L.; Ericson, J.; Sander, M.; Simeone, A.; et al. Nkx6-1 controls the identity and fate of red nucleus and oculomotor neurons in the mouse midbrain. *Development* **2009**, *136*, 2545–2555. [[CrossRef](#)]
10. Cai, J.; Xu, X.; Yin, H.; Wu, R.; Modderman, G.; Chen, Y.; Qiu, M. Evidence for the differential regulation of Nkx-6.1 expression in the ventral spinal cord and foregut by Shh-dependent and-independent mechanisms. *Genesis* **2000**, *27*, 6–11. [[CrossRef](#)]
11. Schaffer, A.E.; Freude, K.K.; Nelson, S.B.; Sander, M. Nkx6 transcription factors and Ptf1a function as antagonistic lineage determinants in multipotent pancreatic progenitors. *Dev. Cell* **2010**, *18*, 1022–1029. [[CrossRef](#)]
12. Zhou, Q.; Law, A.C.; Rajagopal, J.; Anderson, W.J.; Gray, P.A.; Melton, D.A. A multipotent progenitor domain guides pancreatic organogenesis. *Dev. Cell* **2007**, *13*, 103–114. [[CrossRef](#)]
13. Nelson, S.B.; Schaffer, A.E.; Sander, M. The transcription factors Nkx6.1 and Nkx6.2 possess equivalent activities in promoting beta-cell fate specification in Pdx1+ pancreatic progenitor cells. *Development* **2007**, *134*, 2491–2500. [[CrossRef](#)]
14. Sander, M.; Sussel, L.; Connors, J.; Scheel, D.; Kalamaras, J.; Cruz, F.D.; German, M. Homeobox gene Nkx6. 1 lies downstream of Nkx2. 2 in the major pathway of beta-cell formation in the pancreas. *Development* **2000**, *127*, 5533–5540. [[PubMed](#)]
15. Schisler, J.C.; Fueger, P.T.; Babu, D.A.; Hohmeier, H.E.; Tessem, J.; Lu, D.; Becker, T.C.; Naziruddin, B.; Levy, M.; Mirmira, R.G.; et al. Stimulation of human and rat islet  $\beta$ -cell proliferation with retention of function by the homeodomain transcription factor Nkx6.1. *Mol. Cell. Biol.* **2008**, *28*, 3465–3476. [[CrossRef](#)] [[PubMed](#)]
16. Tessem, J.; Moss, L.G.; Chao, L.C.; Arlotto, M.; Lu, D.; Jensen, M.V.; Stephens, S.B.; Tontonoz, P.; Hohmeier, H.E.; Newgard, C.B. Nkx6.1 regulates islet -cell proliferation via Nr4a1 and Nr4a3 nuclear receptors. *Proc. Natl. Acad. Sci. USA* **2014**, *111*, 5242–5247. [[CrossRef](#)] [[PubMed](#)]
17. Øster, A.; Jensen, J.; Serup, P.; Galante, P.; Madsen, O.D.; Larsson, L.-I. Rat endocrine pancreatic development in relation to two homeobox gene products (Pdx-1 and Nkx 6.1). *J. Histochem. Cytochem.* **1998**, *46*, 707–715. [[CrossRef](#)] [[PubMed](#)]
18. Liu, J.; Hunter, C.S.; Du, A.; Ediger, B.; Walp, E.; Murray, J.; Stein, R.; May, C.L. Islet-1 regulates arx transcription during pancreatic islet  $\alpha$ -cell development. *J. Biol. Chem.* **2011**, *286*, 15352–15360. [[CrossRef](#)] [[PubMed](#)]
19. Schaffer, A.E.; Taylor, B.L.; Benthuyzen, J.R.; Liu, J.; Thorel, F.; Yuan, W.; Jiao, Y.; Kaestner, K.H.; Herrera, P.L.; Magnuson, M.A.; et al. Nkx6.1 controls a gene regulatory network required for establishing and maintaining pancreatic beta cell identity. *PLoS Genet.* **2013**, *9*, e1003274. [[CrossRef](#)] [[PubMed](#)]
20. Jensen, J.; Serup, P.; Karlsen, C.; Nielsen, T.F.; Madsen, O.D. mRNA profiling of rat islet tumors reveals Nkx 6.1 as a  $\beta$ -cell-specific homeodomain transcription factor. *J. Biol. Chem.* **1996**, *271*, 18749–18758. [[CrossRef](#)]
21. Taylor, B.L.; Liu, F.-F.; Sander, M. Nkx6.1 is essential for maintaining the functional state of pancreatic beta cells. *Cell Rep.* **2013**, *4*, 1262–1275. [[CrossRef](#)]
22. Guo, L.; Inada, A.; Aguayo-Mazzucato, C.; Hollister-Lock, J.; Fujitani, Y.; Weir, G.C.; Wright, C.V.; Sharma, A.; Bonner-Weir, S. PDX1 in ducts is not required for postnatal formation of  $\beta$ -cells but is necessary for their subsequent maturation. *Diabetes* **2013**, *62*, 3459–3468. [[CrossRef](#)] [[PubMed](#)]
23. Talchai, C.; Xuan, S.; Lin, H.V.; Sussel, L.; Accili, D. Pancreatic  $\beta$  cell dedifferentiation as a mechanism of diabetic  $\beta$  cell failure. *Cell* **2012**, *150*, 1223–1234. [[CrossRef](#)] [[PubMed](#)]
24. Spracklen, C.N.; Horikoshi, M.; Kim, Y.J.; Lin, K.; Bragg, F.; Moon, S.; Suzuki, K.; Tam, C.H.T.; Tabara, Y.; Kwak, S.-H.; et al. Identification of type 2 diabetes loci in 433,540 East Asian individuals. *Nat. Cell Biol.* **2020**, *582*, 240–245. [[CrossRef](#)]
25. Suzuki, K.; Akiyama, M.; Ishigaki, K.; Kanai, M.; Hosoe, J.; Shojima, N.; Hozawa, A.; Kadota, A.; Kuriki, K.; Naito, M.; et al. Identification of 28 new susceptibility loci for type 2 diabetes in the Japanese population. *Nat. Genet.* **2019**, *51*, 379–386. [[CrossRef](#)]
26. Yokoi, N.; Kanamori, M.; Horikawa, Y.; Takeda, J.; Sanke, T.; Furuta, H.; Nanjo, K.; Mori, H.; Kasuga, M.; Hara, K.; et al. Association studies of variants in the genes involved in pancreatic -cell function in type 2 diabetes in Japanese subjects. *Diabetes* **2006**, *55*, 2379–2386. [[CrossRef](#)]

27. Soriano, P. Generalized lacZ expression with the ROSA26 Cre reporter strain. *Nat. Genet* **1999**, *21*, 70–71. [[CrossRef](#)]
28. Genové, G.; Glick, B.S.; Barth, A.L. Brighter reporter genes from multimerized fluorescent proteins. *Biotechniques* **2005**, *39*, 814–822. [[CrossRef](#)]
29. Copeland, N.G.; Jenkins, N.A.; Court, D.L. Recombineering: A powerful new tool for mouse functional genomics. *Nat. Rev. Genet.* **2001**, *2*, 769–779. [[CrossRef](#)]
30. Hsu, P.D.; Scott, D.A.; Weinstein, A.J.; Ran, F.A.; Konermann, S.M.; Agarwala, V.; Li, Y.; Fine, E.J.; Wu, X.; Shalem, O.; et al. DNA targeting specificity of RNA-guided Cas9 nucleases. *Nat. Biotechnol.* **2013**, *31*, 827–832. [[CrossRef](#)]
31. Hitz, C.; Wurst, W.; Kühn, R. Conditional brain-specific knockdown of MAPK using Cre/loxP regulated RNA interference. *Nucleic Acids Res.* **2007**, *35*, e90. [[CrossRef](#)] [[PubMed](#)]
32. Bastidas-Ponce, A.; Tritschler, S.; Dony, L.; Scheibner, K.; Tarquis-Medina, M.; Salinno, C.; Schirge, S.; Burtscher, I.; Böttcher, A.; Theis, F.J.; et al. Comprehensive single cell mRNA profiling reveals a detailed roadmap for pancreatic endocrinogenesis. *Development* **2019**, *146*, dev173849. [[CrossRef](#)] [[PubMed](#)]
33. Burtscher, I.; Lickert, H. Foxa2 regulates polarity and epithelialization in the endoderm germ layer of the mouse embryo. *Development* **2009**, *136*, 1029–1038. [[CrossRef](#)] [[PubMed](#)]
34. Renier, N.; Wu, Z.; Simon, D.J.; Yang, J.; Ariel, P.; Tessier-Lavigne, M. iDISCO: A simple, rapid method to immunolabel large tissue samples for volume imaging. *Cell* **2014**, *159*, 896–910. [[CrossRef](#)] [[PubMed](#)]